Monitoring DNA/Poly-L-Lysine Polyplex Formation with Time-Resolved Multiangle Laser Light Scattering

Eva Lai* and John H. van Zanten†

*Department of Chemical Engineering, Johns Hopkins University, Baltimore, Maryland 21218, and †Chemical Engineering Department, North Carolina State University, Raleigh, North Carolina 27695-7905 USA

ABSTRACT Nonviral DNA complexes show promise as alternative and attractive gene delivery vectors for treating genetic diseases. Nonviral DNA complexes are typically formed by combining DNA with various condensing/complexing agents such as lipids, polyelectrolytes, polymers, polypeptides, and surfactants in solution. DNA/poly-L-lysine polyplex formation kinetics are probed by time-resolved multiangle laser light scattering (TR-MALLS), which yields the time evolution of the supramolecular complex mass and geometric size. Primary polyplexes whose geometric size is smaller than individual DNA molecules in solution are formed very rapidly upon mixing DNA and poly-L-lysine. Over time, these primary polyplexes aggregate into larger structures whose ultimate size is determined primarily by the relative concentrations of DNA and poly-L-lysine. This final polyplex size varies with the DNA/poly-L-lysine mass ratio in a non-monotonic fashion, with the maximum polyplex size occurring at a DNA/poly-L-lysine mass ratio of approximately two to three (charge ratio near unity). The utility of TR-MALLS for monitoring the temporal evolution of DNA loading and supramolecular complex size growth (mean square radius and molar mass) throughout the DNA/poly-L-lysine polyplex formation process is demonstrated. The polyplex DNA loading and size, both geometric and molar mass, are key to understanding the transfection process and for developing optimal gene therapy vectors.

INTRODUCTION

The past few years have seen a revival of interest in DNA condensation phenomena. The main driving force for these studies has been a growing interest in developing nonviral gene delivery vectors. Many early studies focused on condensing a single DNA molecule to replicate the native DNA structures found in viruses (Bloomfield, 1998). The observed condensates are typically found to be toroids with an average diameter ranging from 25 to 300 nm, and occasionally as rods with average length ranging from 40 to 80 nm. Wilson and Bloomfield (1979) have predicted and experimentally confirmed that DNA in aqueous solution condenses (through intramolecular chain interactions) when 89–90% of the DNA phosphate charge in aqueous solution is neutralized. Other studies have demonstrated that in vitro DNA condensation can be attained by a variety of positively charged polypeptides and proteins, inert polymers and alcohols, and recently, positively charged lipids or liposomes (Gosule and Schellman, 1976; Olins and Olins, 1971; Lerman, 1971; Laemmli, 1975; Wilson and Bloomfield, 1979; Felgner et al., 1987; Koltover et al., 1998).

Growing interest in developing DNA supramolecular complexes for nonviral gene therapy applications has reinvigorated this field. Most studies of nonviral gene delivery systems focus on new condensing agent synthesis (Felgner et al., 1994; Wheeler et al., 1996; Liu et al., 1997, expression vector development (Liang et al., 1996; Kwoh et al., 1999), physicochemical characterization (Mahato et al., 1995; Tomlinson and Rolland, 1996; Duguid et al., 1998), and supramolecular complex structural details (Sternberg et al., 1994; Lasic et al., 1997; Radler et al., 1997; Koltover et al., 1998) with little or no regard to the supramolecular complex formation kinetics. Because the primary goal of the complexation process is to produce a DNA complex dispersion of optimal size and composition, an understanding of the underlying kinetic processes is essential to achieve such a formulation. In fact, Bloomfield (1991) has pointed out that the size distribution of condensed particles may be determined kinetically rather than thermodynamically. Furthermore, the complexation process often promotes further aggregation of the primary condensates (Widom and Baldwin, 1980, 1983; Tomlinson and Rolland, 1996; Perales et al., 1994; Zuidam and Barenholz, 1998). This aggregation phenomenon, a necessary prerequisite to forming DNA supramolecular complexes, can become detrimental when the resultant supramolecular complexes become too large for effective gene delivery. Therefore, studying the supramolecular complexation process, especially its kinetic aspects, is important, and a better understanding may improve the design, control, and formulation of nonviral gene delivery vectors.

Experimental techniques for investigating DNA condensation include direct observation (e.g., electron microscopy), hydrodynamic methods (e.g., centrifugation, dynamic light scattering), optical probes (e.g., circular dichroism, static light scattering), x-ray diffraction, biochemical assays (e.g., enzymatic action of gyrases, endonucleases, polymerases), and ligand binding studies (e.g., heat of interaction, helix-coil transitions, equilibrium dialysis). Of these techniques,

Received for publication 6 June 2000 and in final form 25 October 2000.

Address reprint requests to Dr. John H. van Zanten, Chemical Engineering Department, North Carolina State University, Box 7905, Raleigh, NC 27695. Tel.: 919-515-2520; Fax: 919-515-3465; E-mail: john_vz@ncsu.edu.

0006-3495/01/02/864/10 $2.00

only fluorescence microscopy, dynamic light scattering, and static light scattering can provide real-time monitoring of the complexation processes. Of these, time-resolved multiangle laser light scattering (TR-MALLS) is best suited to monitoring kinetic processes, as it yields both molar masses and geometric sizes in a model-independent manner at high temporal resolution. This report illustrates the utility of TR-MALLS for monitoring DNA complexation kinetic processes noninvasively and in real time. This technique is capable of resolving both long-time aggregation phenomena and the formation of primary condensates at early times, owing to its sensitivity to both DNA complex molar mass and geometric size. This information is particularly relevant for delineating current theories for DNA complex structures (Bruinsma, 1998; Dan, 1998; Harries et al., 1998; Park et al., 1998; Nguyen et al., 2000) and future kinetic models.

In the report that follows it is demonstrated that polyplex molar mass, geometric size, and formation kinetics are primarily determined by relative amounts of DNA and poly-L-lysine. It is shown that at high and low DNA/poly-L-lysine mass concentration ratios, both polyplex molar mass and geometric size remain fairly constant with time after initial aggregation, indicating that aggregation is very rapid and yields polyplexes that remain remarkably stable for at least several hours. It is also observed that at intermediate DNA/poly-L-lysine mass concentration ratios (one to five), the supramolecular molar mass and geometric size increase over several hours, with the maximum size occurring for a DNA/poly-L-lysine mass concentration ratio near two to three (near a charge ratio of unity). Because the DNA molecular weight is 1.8×10^6 g/mol, the high final polyplex molar masses (ranging from 8×10^6 to nearly 5×10^9 g/mol) are due to primary polyplex aggregation. Hence, each polyplex contains more than one DNA molecule, as observed for other DNA condensation or complexation processes (Arscott et al., 1990; Bloomfield et al., 1992; Pitard et al., 1997). The final polyplexes are stable and do not precipitate out of solution at these high molar masses.

MATERIALS AND METHODS

Materials

Ultra-pure HEPES (Gibco Life Technologies, Gaithersburg, MD) was dissolved in deionized water and the pH was adjusted by adding NaOH. Poly-L-lysine (Sigma, St. Louis, MO) of molecular mass 15–30 kDa, 75–150 kDa, and >300 kDa was used as received from the vendor without further purification or modification. Stock solutions for each poly-L-lysine molecular weight were prepared by weighing and then dissolving a given mass in 20 mM HEPES (pH 7.45) which had been polished with a 0.1-μm pore size membrane filter. All other solutions were prepared from these stock solutions.

DNA amplification and purification

Plasmid DNA (pUC19, 2.7 kbp) was amplified in DH5α competent cells according to the vendor's instructions (Gibco Life Technologies). The plasmid DNA was purified by phenol/chloroform extraction and ethanol precipitation. The dried pellet was dissolved in 20 mM HEPES solution (pH 7.45). The nucleic acid concentration and purity were measured by UV absorption at 260, 270, and 280 nm. The occurrence of pUC19 plasmids was verified by electrophoresis on 1% agarose gel. More than 90% of the resultant plasmids were found to be supercoiled.

Refractive index increment measurements

The refractive index increments for each poly-L-lysine molecular weight and the pUC19 plasmid DNA were measured independently using an Optilab DSP Interferometric Refractometer (Wyatt Technology Inc., Santa Barbara, CA). Measurements were conducted off-line at a wavelength of 632.8 nm in vacuo. The temperature was set at 40°C to minimize fluctuations. To avoid contaminants, both the sample and reference cells were washed with 6 ml of 6 N HNO_3 and rinsed with 10 ml of deionized water. For each poly-L-lysine and DNA considered here, at least seven different concentrations were prepared from the same batch of 0.1-μm filtered solvent (20 mM HEPES at pH = 7.45) and stock solution. This sample preparation method avoids any inconsistency between samples other than those attributed to the solute itself. The concentration was determined by weighing both the amount of solvent and stock solution. This approach ensures that the solution concentrations are known to at least 1% accuracy. Clean solvent was injected before and after each refractive index determination to confirm the baseline voltage and check for baseline drift. The experimentally measured refractive index increments for each solute considered here are shown in Table 1. The refractive index increments of the two lower-molecular-weight poly-L-lysines and the plasmid DNA are essentially the same. Somewhat alarming is the refractive index increment measured for the highest-molecular-weight poly-L-lysine. The measured value was reproduced several times. This lower value may be a result of sample contamination, as the poly-L-lysine was used as received from the vendor without further purification.

Time-resolved multiangle laser light-scattering measurements

TR-MALLS measurements were performed with a DAWN DSP Laser Photometer (Wyatt Technology Inc.). The instrument is equipped with 18 fixed photodiode detectors at angular positions ranging from 22.5° to 147.0°. The light source is a vertically polarized 5 mW He-Ne laser with a wavelength of 632.8 nm in vacuo.

Complexation reactions were carried out in 20-ml glass scintillation vials, which were carefully cleaned, rinsed with filtered deionized water, and dried to eliminate any contaminants, including dust and ions. Solvent was cleaned with a 0.1-μm pore size Anotop Whatman (VWR, Baltimore, MD) syringe filter to eliminate dust. Also, dust contaminants in the DNA stock solution were removed by a 0.2-μm polysulfone centrifuge filter (Whatman, Clifton, NJ) and the DNA concentration was determined before and after filtration. The polysulfone membranes exhibit low protein binding affinity and the 0.2 μm pore size is on the order of the actual hydrated DNA size. Before each experiment, the makeup solvent was checked for clarity by measuring its background scattering at very low angles and a sample was discarded if the background noise was unacceptable. These

TABLE 1 Refractive index increment values

Solute	$\partial n/\partial c$ (ml/g)
Poly-L-lysine >300 kDa	0.1490 ± 0.0001
Poly-L-lysine 75–150 kDa	0.1679 ± 0.0002
Poly-L-lysine 15–30 kDa	0.1696 ± 0.0008
Plasmid DNA	0.1705 ± 0.0031

precautions in sample preparation are necessary to minimize artifacts owing to dust contamination. DNA/poly-L-lysine complexation was initiated by adding the appropriate poly-L-lysine concentration to a solution of fixed DNA concentration (12.6 μg/ml or 4 μg/ml). The total reaction volume was 5 ml. The solution was gently mixed for a couple of seconds to avoid bubble formation before measurement. The complexation process was monitored for ~2.5 h, with light-scattering spectra being collected every 1 or 6 s. All measurements were conducted at ~30°C.

Traditionally, static light scattering has been used to determine the geometric size and molar mass of macromolecules and particles in solution among other applications. The Rayleigh-Gans-Debye approximation for scattering from a dilute dispersion of optically isotropic solutes varying in size and composition can be expressed most generally by the excess Rayleigh ratio, R_θ, which is directly proportional to the light scattered by solutes dispersed in a solvent, as follows (Berry, 1987)

$$R_\theta = K'\psi^2_{\text{solute}} c M_{\text{LS}} P_{\text{LS}}(\theta), \tag{1}$$

where c is the total mass concentration, M_{LS} is a light-scattering average molar mass or the apparent molar mass as measured by light-scattering, $P_{\text{LS}}(\theta)$ is a light-scattering average intraparticle interference factor that provides a measure of the mass distribution within a given solute, and ψ_{solute} is the contrast factor which, in the case of light scattering, is the so-called refractive index increment, $(\partial n/\partial c)$, and it is given by $\Sigma_\mu\, w_\mu \psi_\mu$, where w_μ is the weight fraction of solute type μ and ψ_μ is the corresponding solute's refractive index increment. K' is an optical constant, $K' = 4\pi^2 n_o^2 / N_A \lambda_o^4$, where n_o is the refractive index of the pure solvent, N_A is Avogadro's number, and λ_o is the wavelength of the incident light in vacuo. The treatment presented here is exact only in the limit of an infinitely dilute solution, as interparticle interactions have been neglected. However, for the case of sufficiently dilute solutions, interparticle interactions can be safely ignored and expression (1) is still applicable. The usual approach taken for polymer solutions is to collect a series of spectra at varying concentrations and extrapolate to zero solute concentration to yield the corresponding infinite dilution spectra. For the study presented here, the greatest solute concentration is $\sim 5 \times 10^{-5}$ g/ml (which is sufficiently dilute to neglect interparticle interactions) and thus, dilution is unnecessary. This is fortunate, as supramolecular complexes may be structurally and compositionally altered following dilution.

The light scattering average molar mass accounts for the fact that heterogeneous particles such as supramolecular complexes are composed of scattering units of varying weight *and* optical contrast. Therefore, the apparent molar mass determined from light scattering is a measure of the total scattering power present in the particle. However, if each particle is compositionally homogeneous or when each scattering element has the same refractive index increment, the light-scattering averaged molar mass is simply the weight-averaged molar mass, M_w. Although the condition of equal refractive index increments will not be true in general, for the DNA/poly-L-lysine polyplexes considered herein the condition is nearly satisfied (see Table 1).

As noted previously, the light-scattering average intraparticle interference factor provides a measure of the intraparticle scattering element distribution. The intraparticle interference factor is expressed in the following manner,

$$P_{\text{LS}}(\theta) = 1 - \frac{q^2 \langle r^2 \rangle_{\text{LS}}}{3!} + O(q^4). \tag{2}$$

Here $\langle r^2 \rangle_{\text{LS}}$ denotes a light-scattering average mean-square radius and $q = 4\pi n_o/\lambda_o \sin(\theta/2)$ is the scattering vector at scattering angle θ. The mean-square radius and so-called radius of gyration, R_G, can be related through the mathematical expression: $\langle r^2 \rangle = 2R_G^2$. In general, the light-scattering average radius of gyration is a multifaceted quantity that depends on both the mass and optical contrast spatial distributions within a particle. For the special case wherein the scattering elements have the same refractive index increment, the light-scattering averaged mean-square radius is greatly simplified

$$\langle R_G^2 \rangle_{\text{LS}} = \frac{\sum_\mu w_\mu M_\mu \langle R_G^2 \rangle_\mu}{M_w}. \tag{3}$$

Higher-order radius moments can be used to monitor in more detail the size distribution changes, which occur throughout the aggregation process (Lai and van Zanten, manuscript in preparation).

RESULTS AND DISCUSSION

When considering light scattering from DNA/poly-L-lysine solutions, it is necessary to account for the presence of both DNA/poly-L-lysine polyplexes and free poly-L-lysine molecules in solution. Because DNA has a large negative charge density, it is reasonable to assume that nearly all the DNA molecules in solution rapidly combine with the positively charged poly-L-lysine. Hence, very few, if any, free DNA molecules would remain in solution after mixing with poly-L-lysines. The excess Rayleigh ratio is

$$R_\theta = K'\psi_S^2 c_S M_{S,\text{LS}} P_{S,\text{LS}}(\theta) + K'\psi_P^2 c_P M_{P,\text{LS}} P_{P,\text{LS}}(\theta) \tag{4}$$

where the subscripts S and P denote supramolecular complexes and free poly-L-lysines, respectively. This expression can be greatly simplified by taking the limit $q \to 0$ wherein all $P_{i,\text{LS}}(\theta) \to 1$. The excess Rayleigh ratio at zero angle is given by

$$R_{\theta=0} = K'\psi_S^2 c_S M_{S,\text{LS}} + K'\psi_P^2 c_P M_{P,\text{LS}}. \tag{5}$$

Although the refractive index increments and solution DNA and condensing agent mass concentrations are usually going to be of similar magnitude, there are many situations in which the supramolecular complex molar mass will be much larger than the condensing agent molar mass. In general, the primary condensate consists of two to hundreds of DNA molecules, while the final supramolecular complex contains several hundreds to thousands of DNA molecules. Therefore, the supramolecular complex molar mass can be several orders of magnitude greater than the poly-L-lysine molar mass. Also, the scattering from free poly-L-lysines at the total solution concentration considered here is only slightly above the background solvent scattering and much less than that of the free DNA itself. Hence, the excess scattered intensity is essentially due to the supramolecular complexes. Under these conditions, the excess Rayleigh ratio at zero angle can be further approximated as

$$R_{\theta=0} \cong K'\psi_S^2 c_S M_{S,\text{LS}}. \tag{6}$$

As noted previously, the scattering contribution of free poly-L-lysines is assumed to be negligible since $c_P M_{P,\text{LS}} \ll c_S M_{S,\text{LS}}$. This limiting expression will be used to interpret the DNA/poly-L-lysine solution light-scattering spectra that

follow. Throughout this report the mass concentration, c_S, will be taken as the sum of the DNA and poly-L-lysine solution concentrations. This assumption will overestimate the supramolecular complex solution concentration and, therefore, underestimate the supramolecular complex molar mass somewhat. However, this effect will not be substantial other than cases wherein the DNA/poly-L-lysine mass ratio is very small. It should be noted that this assumption might not be valid for the case of DNA/lipid lipoplexes wherein the solution may contain both supramolecular complexes and free liposomes of very high molecular weight. When the free complexing agent makes a significant contribution to the excess scattering, fractionation methods followed by light scattering may be preferred (Korgel et al., 1998).

Given a valid intraparticle interference factor, it is a straightforward matter to interpret static light-scattering spectra for monodisperse suspensions of scatterers. However, in general the scatterer geometry is not known. In addition, size polydispersity is often a significant factor. Therefore, several graphical techniques are typically considered when analyzing light-scattering spectra. The most common approaches are those of Debye (R_θ vs. q^2), Zimm (R_θ^{-1} vs. q^2), and Berry ($R_\theta^{-1/2}$ vs. q^2). For typical macromolecular solutions, the Zimm method is the usual choice because it allows a linear extrapolation of the light-scattering spectra (i.e., proportional to q^2) over a greater range of scattering vector values than the Debye method. However, the Zimm method sometimes fails for very large molar masses wherein the zero angle extrapolation can yield negative values, since $R_\theta^{-1} \propto M_{LS}^{-1}$. Therefore, when considering scatterers of very large molar mass the Debye representation is often preferred to that of Zimm. Although the Berry method is often used in the analysis of spectra acquired for solutions containing scatterers of various geometric shape, it is actually only applicable to the case of size and composition monodisperse random coils. The Debye method, and also that of Zimm, requires no assumptions regarding the supramolecular complex shape. In addition, the Debye approach will always yield non-negative molar masses upon extrapolation to zero scattering angle. Hence, this method is the most appropriate choice for the extremely high molar mass scatterers considered here. The weight average molar mass and geometric size estimated by the Debye method are comparable to the other two approaches, as shown in Table 2.

The marked curvature of the light-scattering spectra angular dependence observed at late stages in the complexation process can lead to difficulties in extrapolating to zero scattering angle and determining the supramolecular complex geometric size. For sufficiently small particles, such as those formed at early times, the intraparticle interference factor is essentially linearly proportional to q^2. At later times the spectra begin to exhibit marked curvature at fairly small scattering angles (see Fig. 1). In this case a second-order Debye method is used in which the intraparticle interference factor's q^4 dependence is accounted for in the spectra analysis. This higher-order analysis provides some insight into the dispersion polydispersity, but this discussion will be left for a later communication (Lai and van Zanten, unpublished results). One should note that the truly large molar masses of order 10^9 g/mol and the comparatively small radii indicate the DNA/poly-L-lysine polyplexes are relatively dense, compact structures compared to the native free DNA and poly-L-lysine. For instance, a solid sphere of 100 nm radius and a mass density of 1 g/cc will have a molar mass of $\sim 2.5 \times 10^9$ g/mol.

As outlined previously, the determination of molar masses and radii of gyration requires extrapolating multiangle light-scattering spectra to zero scattering angle. Earlier, the relative merits of the Debye, Zimm, and Berry methods were discussed. Although the authors' rationale for utilizing a second-order Debye fit was outlined, the angular range to be utilized for extrapolation remains an issue. The extrapolation process yields a y-intercept and the limiting slope as $q^2 \rightarrow 0$, from which the weight average molar mass and light-scattering average radius of gyration are calculated, respectively. Three possible Debye fits through various scattering angles are shown in Fig. 1. Table 3 lists the weight average molar masses and light-scattering average radii of gyration obtained for each fit illustrated in Fig. 1. A linear Debye fit through the three lowest scattering angles, 22.5–32°, yields a polyplex molar mass and radius of gyration of $1.55 \pm 0.02 \times 10^9$ g/mol and 114 ± 13 nm, respectively. Although a linear fit through the lowest scattering angles may seem to be the preferred choice, this would use only the three lowest scattering angles. Unfortunately, these low scattering angles are the most susceptible to experimental artifacts and therefore do not always provide a reliable estimate. Therefore, it is preferable to utilize a second-order Debye approach over a greater angular range. The angular ranges (22.5–72°) and (32–72°) yield molar mass and radius of gyration values comparable to those found from the linear Debye fit over the three lowest scattering angles (see Table 3). Because the two lowest scattering angles are susceptible to artifacts owing to dust contamination and stray light, the angular range 32–72° was selected for the second-order Debye analysis used throughout this report. The calculated molar masses and radii of gyration determined from the second-order Debye fits through scattering angles 32–72° almost overlay those obtained by a linear Debye fit of the three lowest scattering angles (data not shown).

TABLE 2 Comparison of analysis methods

Method	M_w (g/mol)	$\langle r^2 \rangle_{LS}$ (nm)
First-order Zimm	$(1.21 \pm 0.03) \times 10^9$	142.3 ± 1.6
Second-order Berry	$(1.08 \pm 0.02) \times 10^9$	114.9 ± 1.1
Second-order Debye	$(1.02 \pm 0.03) \times 10^9$	100.9 ± 6.0

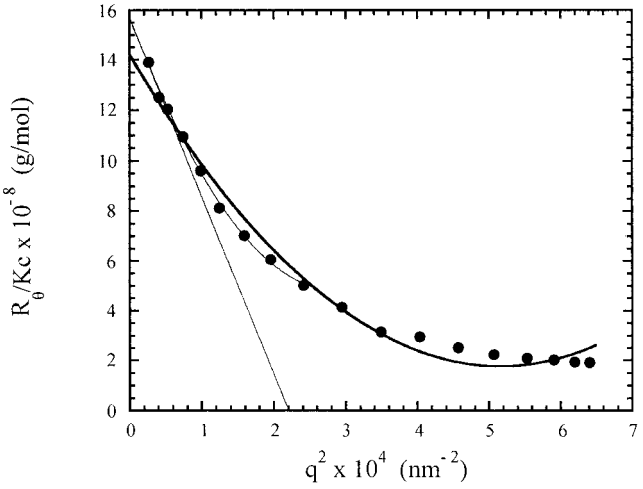

FIGURE 1 A comparison of three different curve fits to the same light-scattering spectra. The bold curve corresponds to a second-order Debye fit through all 18 accessible scattering angles, 22.5–147°. The thin, straight line corresponds to a first-order Debye fit to the three lowest scattering angles, 22.5–32°. The thin curve corresponds to a second-order Debye fit to scattering angles 32–72°. The straight line fit (three lowest accessible scattering angles) and the limited range second-order Debye fit curve essentially overlay one another at small scattering vector values. The DNA/poly-L-lysine solution composition is 4 μg DNA/ml and 1.33 μg poly-L-lysine/ml. The poly-L-lysine molar mass is >300 kDa.

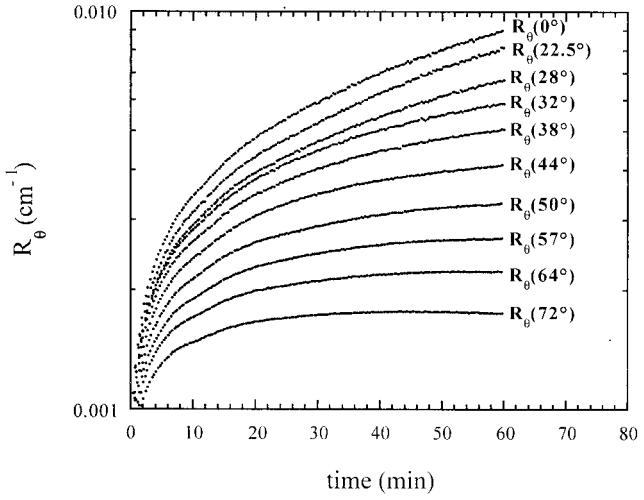

FIGURE 2 Typical light-scattering behavior observed for an aggregating DNA/poly-L-lysine solution. The variation of the excess Rayleigh ratio is displayed as a function of both time and scattering angle. The DNA/poly-L-lysine solution composition is 12.6 μg DNA/ml and 4 μg poly-L-lysine/ml. The poly-L-lysine molar mass is between 75 and 150 kDa.

Typical light-scattering behavior for an aggregating DNA and poly-L-lysine solution is shown in Fig. 2 as the excess Rayleigh ratio versus time at several angles. The reported zero angle Rayleigh ratio is determined from a second-order Debye extrapolation as described previously. Initially the scattered intensity increases very rapidly, especially at the lower angles. Eventually the scattered intensity at nonzero scattering angles passes through a maximum and begins to decrease slowly with time. This temporal behavior is typical of aggregation processes in general. The zero angle Rayleigh ratio provides a measure of the polyplex weight average molar mass, $M_{W,S}$, while the scattered intensity angular dependence is related to the polyplex geometric size. The monotonically increasing zero angle Rayleigh ratio indicates that $M_{W,S}$ is still growing 1 h after mixing. The increasing angular variation of the scattered intensity confirms that the polyplex geometric size is also continuously growing. Initially there is a slight angular dependence because the primary polyplexes formed upon initial mixing are small relative to those formed upon further aggregation. As time proceeds, the supramolecular complex geometric size increases owing to further primary polyplex aggregation (Fig. 5).

TABLE 3 Influence of angular range

Angular Range	M_w (g/mol)	$\langle r^2\rangle_{LS}$ (nm)
22.5°–147°	$(1.39 \pm 0.03) \times 10^9$	99.6 ± 2.6
22.5°–90°	$(1.51 \pm 0.03) \times 10^9$	111.4 ± 2.9
22.5°–72°	$(1.56 \pm 0.02) \times 10^9$	118.6 ± 2.6
32°–72°	$(1.57 \pm 0.02) \times 10^9$	119.0 ± 3.1

The plasmid DNA geometric size (radius of gyration, R_G) and molar mass have been measured independently by light scattering to be 169 ± 6 nm and $1.84 \pm 0.25 \times 10^6$ g/mol, respectively. Using the standard conversion factor for a double-stranded deoxyribonucleic acid (1 kbp = 6.6×10^5 g/mol), the molar mass of a 2.7 kbp DNA is $\sim 1.8 \times 10^6$ g/mol. Thus, the experimental value is in excellent agreement with the calculated theoretical molar mass. For the solution conditions of Fig. 4, the primary polyplex geometric size is ~68 nm, indicating that the primary polyplex is less than one-half the size of free DNA. As time proceeds, the DNA/poly-L-lysine polyplexes grow via secondary aggregation of primary complexes. After 2 h, the polyplex size increases to approximately two and one-half times the initial primary polyplex size. Others have also noted this increase in DNA complex size over time owing to ongoing aggregation processes (Tomlinson and Rolland, 1996; Escriou et al., 1998; Zuidam and Barenholz, 1998).

The temporal dependence of the polyplex molar mass and geometric size is shown in Figs. 5 and 6, respectively. In both figures the DNA concentration is kept constant at 12.6 μg/ml, while the poly-L-lysine concentration (M_w = 75–150 kDa) is varied. Two types of kinetic behavior are observed: 1) continually growing molar mass, or 2) a relatively constant molar mass following a rapid primary complexation process. It is apparent that two distinct regimes exist in the growing molar mass-type kinetics. The first regime is a rapid rise in molar mass wherein the primary polyplexes are formed, followed by the second regime in which the pri-

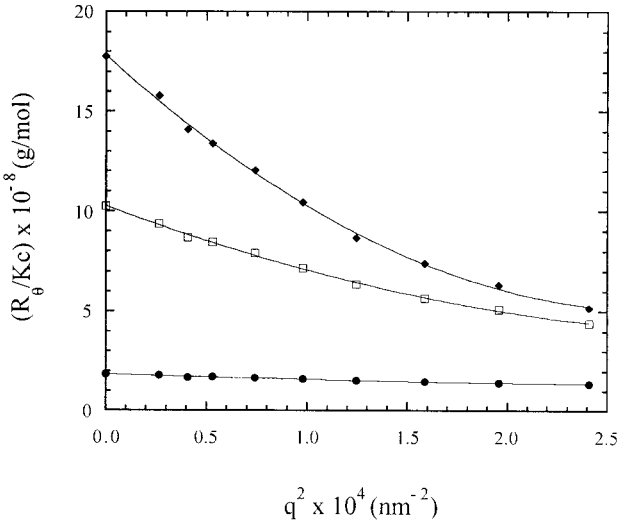

FIGURE 3 Typical light-scattering spectra angular dependence and its change with respect to time observed for an aggregating DNA/poly-L-lysine solution. The curves represent second-order Debye fits to the light-scattering spectra. The aggregation times are (●) 0^+ min, (□) 10 min, and (◆) 30 min. The DNA/poly-L-lysine solution composition is 12.6 μg DNA/ml and 4 μg poly-L-lysine/ml. The poly-L-lysine molar mass is between 75 and 150 kDa.

mary polyplexes undergo further aggregation with one another. Eventually the second regime ceases and the polyplex molar mass and geometric size reach their steady-state values. The growing molar mass kinetic behavior occurs for

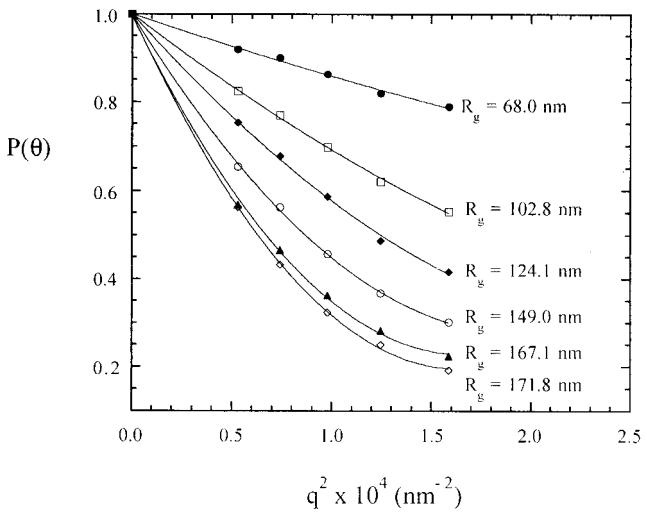

FIGURE 4 Variation of scattered light intensity as a function of scattering angle at various times during the aggregation of DNA and poly-L-lysine. The curves represent a second-order Debye fit to the light-scattering spectra with the corresponding geometric sizes determined from the fit. The times of aggregation are (●) 0^+ min, (□) 10 min, (◆) 30 min, (○) 60 min, (▲) 90 min, and (◇) 120 min. The DNA/poly-L-lysine solution composition is 12.6 μg DNA/ml and 4 μg poly-L-lysine/ml. The poly-L-lysine molar mass is between 75 and 150 kDa.

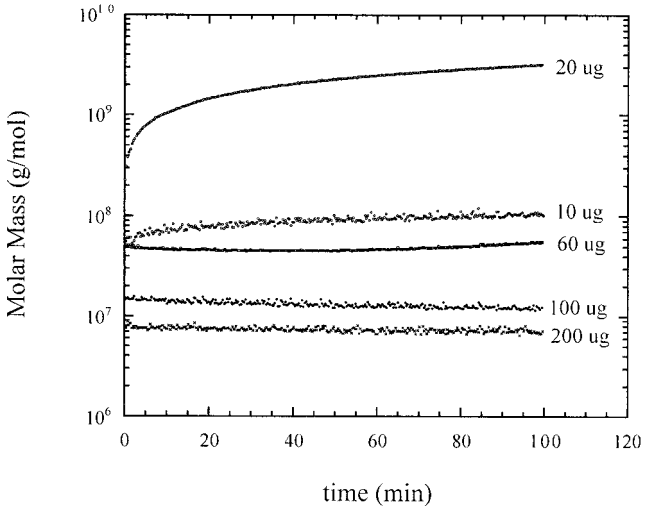

FIGURE 5 Typical polyplex molar mass temporal behavior for an aggregating DNA/poly-L-lysine solution. Listed at the right of each time trace is the poly-L-lysine mass added for each complexation reaction (the reaction volume was 5 ml in each case). The DNA mass is fixed at 12.6 μg/ml and the poly-L-lysine molar mass is between 75 and 150 kDa.

DNA/poly-L-lysine mass concentration ratios ranging from one to five. In fact, this observation is independent of DNA concentration or poly-L-lysine molecular weight. The primary polyplex aggregation is most pronounced for DNA/poly-L-lysine mass concentration ratios ranging from two to three. The polyplex geometric size exhibits very similar behavior. The other observed kinetic behavior, relatively constant molar mass, which indicates rapid formation of stable primary polyplexes, occurs when the poly-L-lysine

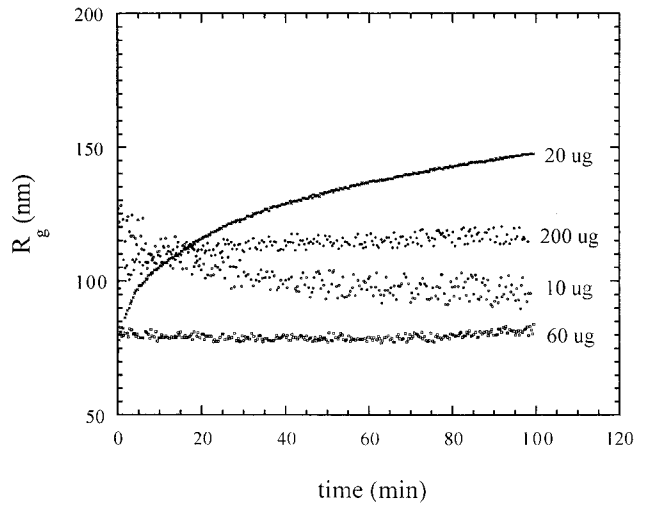

FIGURE 6 Typical polyplex geometric size temporal behavior for an aggregating DNA/poly-L-lysine solution. Listed at the right of each time trace is the poly-L-lysine mass added for each complexation reaction (the reaction volume was 5 ml in each case). The DNA mass is fixed at 12.6 μg/ml and the poly-L-lysine molar mass is between 75 and 150 kDa.

mass concentration exceeds the DNA mass concentration or is much less than the DNA mass concentration. Here, both the polyplex molar mass and geometric size remain relatively stable following initial complexation. However, it is apparent in Fig. 6 that the complexes do undergo some structural rearrangement at near-constant molar mass, especially at very small and very high DNA/poly-L-lysine mass concentration ratios. Stable primary polyplexes are observed for all three poly-L-lysine molecular weights considered at DNA/poly-L-lysine mass concentration ratios below one and above five. One should note that the experimental variation is more prevalent in the radii of gyration determinations (Fig. 6) than the measured molar masses (Fig. 5). This owes to the greater sensitivity of the slope in contrast to the intercept for the second-order Debye fit utilized here.

It was also observed that the poly-L-lysine molecular weight has some influence on the polyplex molar mass growth; further examination of its influence is warranted as to how it dictates the final polyplex molar mass as the DNA/poly-L-lysine mass concentration ratio changes. The final polyplex molar mass is determined when the growth regime has reached a plateau. This usually occurs roughly 2 h after mixing DNA and poly-L-lysine. Based on the previous observation that poly-L-lysine molecular weight has some influence on the polyplex molar mass growth, it is expected that the final polyplex molar mass will vary for each DNA/poly-L-lysine mass concentration ratio (see Fig. 7). The various poly-L-lysine molecular weights yielded different final polyplex molar masses. Interestingly, this variation is reproducibly non-monotonic with poly-L-lysine molecular weight. However, the final polyplex molar masses formed by the various poly-L-lysine molecular weights all displayed a similar trend: the final molar mass depends most strongly on the DNA/poly-L-lysine mass concentration ratio. Note that the largest final polyplex molar mass is formed at a DNA/poly-L-lysine mass concentration ratio near two to three, independent of the poly-L-lysine molecular weight. At this DNA/poly-L-lysine mass concentration ratio, the polyplex formed by the intermediate poly-L-lysine molecular weight produces the smallest geometric size, approximately a 120-nm radius (data not shown).

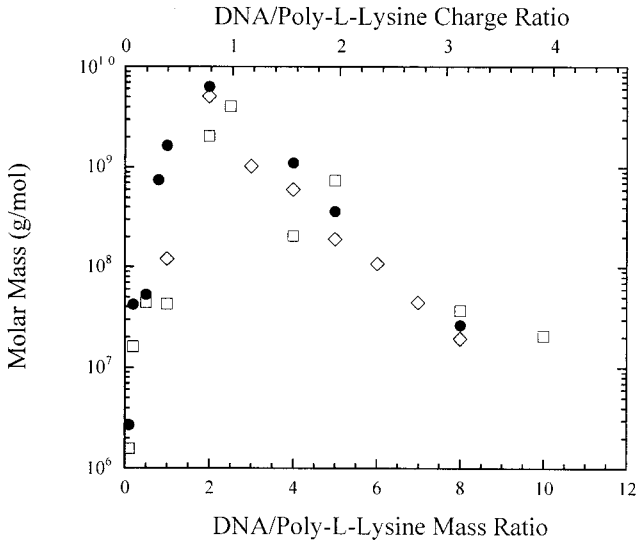

FIGURE 7 DNA/poly-L-lysine polyplex final molar mass as a function of both DNA-to-poly-L-lysine weight ratio (charge ratio) and poly-L-lysine molar mass. The DNA concentration is fixed at 4 μg/ml. The poly-L-lysine molar masses are as follows: (●) 15–30 kDa, (□) 75–150 kDa, and (◇) >300 kDa.

The most interesting observation regarding the polyplex molar mass is the occurrence of its maximum value at a DNA/poly-L-lysine mass concentration ratio near two to three. The experimental measurements indicate that as the poly-L-lysine concentration is increased, the final polyplex molar mass increases until it reaches a maximum value near the mass concentration ratio of two to three and then gradually decreases with increasing poly-L-lysine concentration. This trend most likely owes to the saturation of accessible poly-L-lysine interaction sites along the constituent DNA within each polyplex. The accessible DNA in a DNA/poly-L-lysine polyplex can interact with free poly-L-lysine in the solvent, unbound intracomplex poly-L-lysine, or unbound poly-L-lysine that is a constituent of a different polyplex (i.e., intercomplex interaction). Secondary aggregation of primary polyplexes most likely occurs through the interaction of accessible, unbound DNA in one primary polyplex with unbound, accessible poly-L-lysine in another primary polyplex. At small poly-L-lysine concentrations relative to the DNA concentration the final polyplexes are relatively small and low in molar mass because the primary polyplexes do not contain enough unassociated poly-L-lysine to cause a significant amount of secondary aggregation. A further increase of the poly-L-lysine concentration yields more unassociated poly-L-lysine, which allows for primary polyplex aggregation to occur, leading to larger final polyplex molar masses. The maximum molar mass value is attained when all accessible interaction sites on the surface of the DNA/poly-L-lysine polyplexes are occupied. Additional increases in the poly-L-lysine concentration (beyond a DNA/poly-L-lysine mass concentration ratio near two to three, which is near the isoelectric point) should screen interactions and thereby reduce aggregation of primary polyplexes. This scenario provides a possible explanation of why increasing the poly-L-lysine concentration further results in ever smaller final polyplex molar masses.

Interestingly, although DNA concentration does have some influence on the polyplex final molar mass and geometric size (especially at low DNA/poly-L-lysine mass concentration ratio), it is not in the manner many gene delivery vector developers have assumed. In order to investigate the effect of DNA concentration, polyplexes were prepared at fixed poly-L-lysine molecular weight and concentration while varying only the DNA concentration. Once again, the final molar masses depend strongly on the DNA/poly-L-

lysine mass concentration ratio (see Fig. 8). However, higher DNA concentrations did not lead to higher supramolecular complex molar masses, as is often assumed by vector developers. Both DNA concentrations considered here yielded similar geometric sizes ranging from 75 nm to 160 nm (R_G), but no obvious trends were observed (data not shown). However, DNA concentrations greater than those considered here generally lead to unstable, larger supramolecular complexes (Lai and van Zanten, unpublished results).

For gene therapy, the usual objective is to deliver a large quantity of DNA in the smallest vector possible to achieve a therapeutic effect. Most studies have emphasized solution composition, amount of DNA and, to a lesser extent, vector size as the parameters most influencing successful gene delivery and expression. However, essentially none have developed methods to measure more detailed properties such as the DNA copies per vector, vector composition, or vector dispersion size and composition polydispersity. Focusing on the amount of DNA being delivered, the only parameter typically considered is DNA concentration. It appears to be a standard practice to assume that DNA uptake by cells is determined by the DNA concentration used in the formulation and that increasing DNA concentrations will lead to higher DNA uptake or transfection. However, increasing the DNA concentration leads to a more concentrated DNA complex dispersion, which often produces unacceptably large complexes that are ineffective for delivery, and exhibit increased toxicity. To avoid formulations with undesirable characteristics such as these, a more meaningful and insightful parameter is warranted for better characterization of DNA complexes. Instead of relying on DNA concentration to predict DNA uptake, a new parameter called DNA loading, defined as the number of DNA molecules per supramolecular complex volume, may prove to be more useful for interpreting transfection experiments when considered in tandem with the complex geometric size. This DNA loading parameter is essential for characterizing the physical properties of DNA complexes. Gene delivery vector efficacy, and ultimately efficiency, is closely related to the amount of delivered DNA which is controlled by the supramolecular complex size and composition distribution. Thus, the DNA loading parameter, supramolecular complex geometric size, and gene expression efficiency should be closely correlated. The measurements described here indicate that higher DNA concentrations do not necessarily translate to higher DNA loading (see Fig. 9). Thus, increasing DNA concentration may not always lead to an increase in DNA uptake because higher DNA concentrations generally lead to unacceptably large vector size. Greater transfection efficiencies are expected for DNA supramolecular complexes (i.e., gene delivery vectors) of optimum geometric size, composition, and physicochemical properties that also exhibit significant DNA loading on a per volume basis. In this study the highest DNA loading (corresponding to the most DNA molecules per particle) at the smallest polyplex size is formed by the intermediate molecular weight poly-L-lysine at a DNA/poly-L-lysine mass concentration ratio near two to three. This formulation corresponds to more than a thousand DNA molecules packed together in a particle whose radius of gyration is smaller

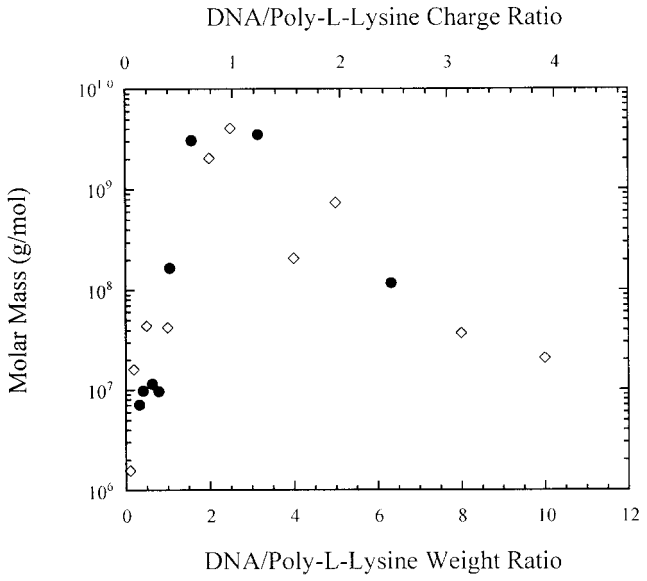

FIGURE 8 DNA/poly-L-lysine polyplex final molar mass as a function of both DNA-to-poly-L-lysine weight ratio (charge ratio) and amount of DNA added. The poly-L-lysine molar mass was between 75 and 150 kDa. The DNA concentrations are (●) 12.6 μg/ml and (◇) 4 μg/ml, respectively.

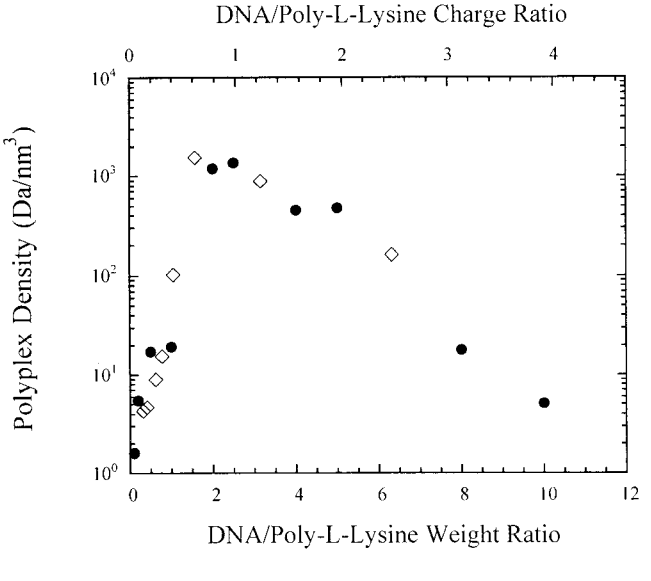

FIGURE 9 DNA/poly-L-lysine final polyplex density as a function of both DNA-to-poly-L-lysine weight ratio (charge ratio) and amount of DNA added. The polyplex density is calculated as $M_{LS}/\langle R_G^2\rangle_{LS}^{3/2}$. The poly-L-lysine molar mass was between 75 and 150 kDa. The DNA concentrations are 12.6 μg/ml (◇) and 4 μg/ml (●), respectively.

than 120 nm. This DNA/poly-L-lysine mass concentration ratio corresponds to a charge ratio near unity.

CONCLUSIONS

Polyplex molar mass, geometric size, and formation kinetics are primarily determined by the DNA-to-poly-L-lysine mass concentration ratio. At relatively high and low DNA/poly-L-lysine mass concentration ratios, both polyplex molar mass and geometric size remain fairly constant with time after initial aggregation, indicating that aggregation is very rapid and yields polyplexes that remain remarkably stable for at least several hours. At intermediate DNA/poly-L-lysine mass concentration ratios (one to five), the supramolecular molar mass and geometric size increase over several hours. Inasmuch as the DNA molecular weight is 1.8×10^6 g/mol, the high final polyplex molar masses (ranging from 8×10^6 to nearly 5×10^9 g/mol) are due to primary polyplex aggregation. Hence, each polyplex contains more than one DNA molecule, as observed for other DNA condensation or complexation processes (Arscott et al., 1990; Bloomfield et al., 1992; Pitard et al., 1997). The final polyplexes are stable and do not precipitate out of solution at these high molar masses.

Both poly-L-lysine molecular weight and DNA concentration have an effect on the physical properties of the polyplex, such as molar mass and geometric size. However, the final polyplex molar mass is most dependent on the DNA/poly-L-lysine mass concentration ratio, and to a lesser extent on the poly-L-lysine molecular weight. Increasing the DNA concentration at a specific DNA/poly-L-lysine mass concentration ratio does not always augment the number of DNA molecules per polyplex. In some cases, increasing the DNA concentration actually reduces the number of DNA molecule per polyplex. Polyplexes with the greatest DNA loading were found to occur at DNA/poly-L-lysine mass concentration ratios near two to three, which corresponds to a DNA/poly-L-lysine charge ratio near unity.

Time-resolved multi-angle laser light scattering has been demonstrated to provide a means for monitoring DNA/poly-L-lysine aggregation kinetics in real time. Because chemical or physical alterations of sample environment are unnecessary, the complexation process is measured in its true aqueous environment. This rapid, noninvasive technique allows for both supramolecular complex molar mass and geometric size determination without using size standards or assuming a supramolecular complex shape. Furthermore, measurements of the supramolecular complex molar mass and geometric size provide invaluable information that can be used to interpret gene therapy studies and thereby facilitate the development of optimal formulations for various gene delivery systems such as polymer, peptide, and lipid-based vectors.

The authors gratefully acknowledge the support of the National Science Foundation (CTS-9702413) and Valentis, Inc. (Burlingame, CA). The authors also acknowledge the helpful and illuminating comments of the reviewers.

REFERENCES

Arscott, P. G., A.-Z. Li, and V. A. Bloomfield. 1990. Condensation of DNA by trivalent cations. 1. Effects of DNA length and topology on the size and shape of condensed particles. *Biopolymers.* 30:619–630.

Berry, G. C. 1987. Light scattering. *In* Encyclopedia of Polymer Science and Engineering. H. F. Mack, et al., editor. John Wiley and Sons, New York. 721–794.

Bloomfield, V. A. 1991. Condensation of DNA by multivalent cations: considerations on mechanism. *Biopolymers.* 31:1471–1481.

Bloomfield, V. A. 1998. DNA Condensation by multivalent cations: considerations on mechanism. *Biopolymers.* 44:269–282.

Bloomfield, V. A., S. He, A.-Z. Li, and P. G. Arscott. 1992. Light scattering studies of DNA condensation. *In* Laser Light Scattering in Biochemistry. S. E. Harding, D. B. Sattelle, and V. A. Bloomfield, editors. The Royal Society of Chemistry, Cambridge. 320–333.

Bruinsma, R. 1998. Electrostatics of DNA cationic lipid complexes: isoelectric instability. *Eur. Phys. J. B.* 4:75–88.

Dan, N. 1998. The structure of DNA complexes with cationic liposomes—cylindrical or flat bilayers? *Biochim. Biophys. Acta.* 1369:34–38.

Duguid, J. G., C. Li, M. Shi, M. J. Logan, H. Alila, A. Rolland, E. Tomlinson, J. T. Sparrow, and L. C. Smith. 1998. A physicochemical approach for predicting the effectiveness of peptide-based gene delivery systems for use in plasmid-based gene therapy. *Biophys. J.* 74: 2802–2814.

Escriou, V., C. Ciolina, F. Lacroix, G. Byk, D. Scherman, and P. Wils. 1998. Cationic lipid-mediated gene transfer: effect of serum on cellular uptake and intracellular fate of lipopolyamine/DNA complexes. *Biochim. Biophys. Acta.* 1368:276–288.

Felgner, P. L., T. R. Gadek, M. Holm, R. Roman, H. W. Chan, M. Wenz, J. P. Northrop, G. M. Ringold, and M. Danielsen. 1987. Lipofection: a highly efficient lipid-mediated DNA transfection procedure. *Proc. Natl. Acad. Sci. USA.* 84:7413–7417.

Felgner, J. H., R. Kumar, C. N. Sridhar, C. J. Wheeler, Y. J. Tsai, R. Border, P. Ramsey, M. Martin, and P. L. Felgner. 1994. Enhanced gene delivery and mechanism studies with a novel series of cationic lipid formulations. *J. Biol. Chem.* 269:2550–2561.

Gosule, L. C., and J. A. Schellman. 1976. Compact form of DNA induced by spermidine. *Nature.* 259:333–335.

Harries, D., S. May, W. M. Gelbar, and A. Ben-Shaul. 1998. Structure, stability, and thermodynamics of lamellar-DNA-lipid complexes. *Biophys. J.* 75:159–173.

Koltover, I., T. Salditt, J. O. Radler, and C. R. Safinya. 1998. An inverted hexagonal phase of cationic liposome-DNA complexes related to DNA release and delivery. *Science.* 281:78–81.

Korgel, B. A., J. H. van Zanten, and H. G. Monbouquette. 1998. Vesicle size distributions measured by flow field-flow fractionation coupled with multiangle light scattering. *Biophys. J.* 74:3264–3272.

Kwoh, D. Y., C. C. Coffin, C. P. Lollo, J. Jovenal, M. G. Banaszczyk, P. Mullen, A. Phillips, A. Amini, J. Fabrycki, R. M. Bartholomew, S. W. Brostoff, and D. J. Carlo. 1999. Stabilization of poly-L-lysine/DNA polyplexes for in vivo gene delivery to the liver. *Biochim. Biophys. Acta.* 1444:171–190.

Laemmli, U. K. 1975. Characterization of DNA condensates induced by poly(ethylene oxide) and polylysine. *Proc. Natl. Acad. Sci. USA.* 72: 4288–4292.

Lasic, D. D., H. Strey, M. C. A. Stuart, R. Podgornik, and P. M. Fredick. 1997. The structure of DNA-liposome complexes. *J. Am. Chem. Soc.* 119:832–833.

Lerman, L. S. 1971. A transition to a compact form of DNA in polymer solutions. *Proc. Natl. Acad. Sci. USA.* 68:1886–1890.

Liang, X., J. Hartikka, L. Sukhu, M. Manthorpe, and P. Hobart. 1996. Novel, high-expressing and antibiotic-controlled plasmid vectors designed for use in gene therapy. *Gene Ther.* 3:350–356.

Liu, Y., L. C. Mounkes, H. D. Liggit, C. S. Brown, I. Solodin, T. D. Heath, and R. J. Debs. 1997. Factors influencing the efficiency of cationic liposome-mediated intravenous gene delivery. *Nat. Biotechnol.* 15: 167–173.

Mahato, R. I., K. Kawabata, T. Nomura, Y. Takakura, and M. Hasida. 1995. Physicochemical and pharmacokinetics characteristics of plasmid DNA/cationic liposome complexes. *J. Pharm. Sci.* 84:1267–1271.

Nguyen, T. T., I. Rouzina, and B. Shklovskii. 2000. Reentrant condensation of DNA induced by multivalent counterions. *J. Chem. Phys.* 112: 2562–2568.

Olins, D. E., and A. L. Olins. 1971. Model nucleohistones: the interaction of F1 and F2al histones with native T7 DNA. *J. Mol. Biol.* 57:437–455.

Park, S. Y., D. Harries, and W. M. Gelbart. 1998. Topological defects and the optimum size of DNA condensates. *Biophys. J.* 75:714–720.

Perales, J. C., T. Ferkol, H. Beegen, O. D. Ratnoff, and R. W. Hanson. 1994. Gene transfer in vivo: sustained expression and regulation of genes introduced into the liver by receptor-targeted uptake. *Proc. Natl. Acad. Sci. USA.* 91:4086–4090.

Pitard, B., O. Aguerre, M. Airiau, A.-M. Lachages, T. Boukhnikachvili, G. Byk, C. Dubertret, C. Herviou, D. Scherman, and J.-F. Mayaux. 1997. Virus-sized self-assembling lamellar complexes between plasmid DNA and cationic micelles promote gene transfer. *Proc. Natl. Acad. Sci. USA.* 94:14412–14417.

Radler, J. O., I. Koltover, T. Salditt, and C. R. Safinya. 1997. Structure of DNA-cationic liposome complexes: DNA intercalation in multilamellar membranes in distinct interhelical packing regimes. *Science.* 275: 810–814.

Sternberg, B., F. L. Sorgi, and L. Huang. 1994. New structures in complex formation between DNA and cationic liposomes visualized by freeze-fracture electron microscopy. *FEBS Lett.* 356:361–366.

Tomlinson, E., and A. P. Rolland. 1996. Controllable gene therapy pharmaceutics of nonviral gene delivery systems. *J. Control Release.* 39: 357–372.

Wheeler, C. J., P. L. Felgner, Y. J. Tsai, J. Marshall, L. Sukhu, S. G. Doh, J. Hartikka, J. Nietupski, M. Manthorpe, M. Nichols, M. Plewe, X. W. Liang, J. Norman, A. Smith, and S. H. Cheng. 1996. A novel cationic lipid greatly enhances plasmid DNA delivery and expression in mouse lung. *Proc. Natl. Acad. Sci. USA.* 93:11454–11459.

Widom, J., and R. L. Baldwin. 1980. Cation-induced toroidal condensation of DNA. *J. Mol. Biol.* 144:431–453.

Widom, J., and R. L. Baldwin. 1983. Monomolecular condensation of l-DNA induced by cobalt hexamine. *Biopolymers.* 22:1595–1620.

Wilson, R. W., and V. A. Bloomfield. 1979. Counterion-induced condensation of deoxyribonucleic acid. A light-scattering study. *Biochemistry.* 18:2192–2196.

Zuidam, N. J., and Y. Barenholz. 1998. Electrostatic and structural properties of complexes involving plasmid DNA and cationic lipids commonly used for gene delivery. *Biochim. Biophys. Acta.* 1368:115–128.